RAPID COMMUNICATIONS

PHYSICAL REVIEW B VOLUME 41, NUMBER 1 1 JANUARY 1990

Evidence for the heavy-fermion normal state of high-temperature superconductors from the theory of spectroscopy

P. C. Pattnaik and D. M. Newns

IBM Research Division, Thomas J. Watson Research Center, P.O. Box 218, Yorktown Heights, New York 10598

(Received 17 March 1989; revised manuscript received 1 November 1989)

We show that recent angle-resolved photoemission and inverse photoemission spectra of $Bi_2Sr_2CaCu_2O_8$ agree well with a numerical theory with no adjustable parameters based on the heavy-fermion normal state. The band structure deduced from the angle-resolved photoemission is in essential accord with the calculation. The three most obvious features of the inverse photoemission spectrum, the Fermi edge, the large width of the empty portion of the band, and the satellite at 2–3 eV, are in agreement with the calculation. These agreements support the heavy-fermion state as the normal state of this material.

The apparently anomalous properties (e.g., resistivity linear with T and Hall coefficient scaling with doping) of the normal state of the high-temperature superconductors have led to many proposals[1,2] as to the non-Fermi-liquid nature of these systems. On the contrary, the present paper argues that evidence from one-electron spectroscopies favors the Fermi-liquid picture. A realistic assessment of the pairing mechanism is impossible until a consensus on the nature of the normal state is achieved.

When the Fermi-liquid picture takes account of the large Coulomb interaction U of 6–8 eV within the Cu d orbitals, and of the significant "oxide gap" of 1–2 eV between the $d^9 2p^6$ and $d^{10} 2p^5$ configurations, it becomes more specifically the "heavy-fermion" state.[3–5] In this state the mass enhancement is ~ 7, consistent with the measured specific heat and susceptibility,[4,5] while the dd charge susceptibility is $\sim \frac{1}{20}$ of the spin susceptibility (i.e., it is deenhanced). The last result is consistent with the fact that in p-type high T_c's the added holes go into the O $2p$ orbitals.[4,5] The recently discovered n-type superconductors can readily be fitted into the heavy-fermion picture, in which the role of doping x is merely to break up the Mott insulating state, and the heavy-fermion Fermi surface contains $1+x$ holes in p-type, and $1-x$ holes in n-type, high T_c's.

Undoubtably the most direct experimental test of the normal state is the one-particle Green's function. The spectral density of this Green's function can be sampled in photoemission and inverse photoemission spectroscopies, with resolutions approaching 20 meV, less than the energy scale of the superconductivity ($2\Delta \sim 60$ meV). Three features of the data seem to show obvious evidence of Fermi-liquid behavior: the sharp Fermi edge,[6,7] the existence of dispersing quasiparticle bands,[6] and the large width of the empty band seen in inverse photoemission.[7] The width of the empty part of the band (1.5 eV) is such that, except in the improbable case of mass enhancement less than unity, it signals the presence of (1+doping) itinerant holes, i.e., the Cu spins are itinerant. A trivial estimate demonstrates this. Taking a free hole gas in two dimensions (2D) with the free-electron mass, and assuming a doping of 21%, if its concentration is the doping, the empty band width is 0.3 eV; if it is (1+doping), the width is 1.5 eV. The itinerant behavior of the Cu spins, which this result demonstrates, is characteristic of the Fermi-liquid picture.

In this paper, we discuss another feature of the inverse photoemission spectrum, a satellite at 2.8 eV, for which there is evidence that it is intrinsic to the planes.[8] We calculate this satellite and show that it is an interband satellite characteristic of the heavy-fermion state. It is interesting to start with a comparison of the calculated[5] heavy-fermion bands with the data of Ref. 6, providing additional evidence for the Fermi-liquid state.

Let us start from the Anderson lattice model of Ref. 4, which gives an approximate description of the CuO_2 planar subsystem which is believed to be the essential active component in the high-temperature superconductors,

$$\mathcal{H} = \sum_{\mathbf{k}\sigma} \epsilon_{\mathbf{k}} c^{\dagger}_{\mathbf{k}\sigma} c_{\mathbf{k}\sigma} + E_1 \sum_{i\sigma} D^{\dagger}_{i\sigma} D_{i\sigma} + \sum_{\mathbf{k}i\sigma} (V_{\mathbf{k}} D^{\dagger}_{i\sigma} c_{\mathbf{k}\sigma} e^{i\mathbf{k}\cdot\mathbf{r}_i} + \text{H.c.}) + U \sum_i N_{di\sigma} N_{di-\sigma} . \quad (1)$$

Here the $c_{\mathbf{k}\sigma}$ are fermion operators for holes of spin σ in the O band of Bloch wave vector $\mathbf{k}$ in the first Brillouin zone, and the $D_{i\sigma}$ are fermion operators for spin-σ holes in the $d_{x^2-y^2}$ orbital on lattice site i, located at $\mathbf{r}_i$. Also, $N_{id\sigma} = D^{\dagger}_{i\sigma} D_{i\sigma}$.

Now since the gap to the d^8-d^9 level is of order 5–7 eV, much larger than the oxide gap, a good approximation for the purposes of this paper is to take this gap as infinite, i.e., take the $U=\infty$ approximation. A rather systematic approach to the $U=\infty$ limit of (1) starts from the slave-boson representation $D_{i\sigma} = b_i^{\dagger} d_{i\sigma}$ of the D-hole operators, where b_i is a boson operator representing the d^{10} state on site i, and $d_{i\sigma}$ is a fermion representing the d^9 state of spin σ on site i. In terms of the slave-boson operators the $U=\infty$ Hamiltonian becomes

$$\mathcal{H} = \sum_{\mathbf{k}\sigma} \epsilon_{\mathbf{k}} c^{\dagger}_{\mathbf{k}\sigma} c_{\mathbf{k}\sigma} + E_1 \sum_{i\sigma} d^{\dagger}_{i\sigma} d_{i\sigma} + \sum_{\mathbf{k}i\sigma} (V_{\mathbf{k}} b_i d^{\dagger}_{i\sigma} c_{\mathbf{k}\sigma} e^{i\mathbf{k}\cdot\mathbf{r}_i} + \text{H.c.}) - \mu \hat{N} + \sum_i \lambda (\hat{Q}_i - 1) , \quad (2)$$

where

$$\hat{N}=\sum_{i\sigma} d_{i\sigma}^{\dagger}d_{i\sigma}+\sum_{\mathbf{k}\sigma} c_{\mathbf{k}\sigma}^{\dagger}c_{\mathbf{k}\sigma}$$

is the global number operator.

It is intrinsic to the slave-boson formulation that the two fields on site i be connected by the local constraint

$$\hat{Q}_i=\sum_{\sigma} d_{i\sigma}^{\dagger}d_{i\sigma}+b_i^{\dagger}b_i=1\,, \tag{3}$$

which, since $[\hat{Q}_i,\mathcal{H}]=0$, conserves probabilities over the boson and fermion subspaces on site i. Remarkably, it is found to be sufficient to impose the constraint of Eq. (3) via a global term involving a Lagrange multiplier λ in Eq. (2). This can be checked by calculating the correlation function of the constraint operator $\langle T\hat{Q}_i(0)\hat{Q}_j(\tau)\rangle$, which turns out to be zero[9,10] to the order we are working, as it should be since the constraint commutes with $\mathcal{H}$. To achieve a more in depth understanding of this, one must reformulate the problem in the radial gauge.[11,12]

The large-N expansion is generated by extending the SU(2) symmetry of spin-$\frac{1}{2}$ to SU(N), and assigning the order of a diagram as a power of $1/N$. Each diagram is given a factor N for each Fermi loop, and a factor $N^{-1/2}$ for each factor $V_{\mathbf{k}}$. The leading N level is achieved by calculating the self-energy in the tadpole diagram approximation. This is equivalent to breaking the local U(1) symmetry of the potential-like gauge field b_i, due to the constraint (3), by introducing the expectation value $\langle b_i\rangle=b$. Then b and the renormalized d level $\epsilon_d=\lambda+E_1$ are solved self-consistently, leading to a mean-field Hamiltonian

$$\begin{aligned}\mathcal{H}'=&\sum_{\sigma}\epsilon_{\mathbf{k}}c_{\mathbf{k}\sigma}^{\dagger}c_{\mathbf{k}\sigma}+\epsilon_d\sum_{i\sigma}d_{i\sigma}^{\dagger}d_{i\sigma}\\&+b\sum_{i\mathbf{k}\sigma}(V_{\mathbf{k}}d_{i\sigma}^{\dagger}c_{\mathbf{k}\sigma}e^{i\mathbf{k}\cdot r_i}+\text{H.c.})\\&+\sum_i(\epsilon_d-F_1)(b^2-1)-\mu\hat{N}\,.\end{aligned} \tag{4}$$

In Fig. 1 we illustrate a renormalized band structure calculated with the extended version of Eqs. (1)–(5) detailed in Ref. 5. This extended model is the same as that just described, but the model is parametrized quantitatively for the entire structure of $La_{2-x}Sr_xCuO_4$, and accurately includes all O $2p$, Cu $3d$, $4s$, and $4p$, and La $5d$ states in the lattice. This model should apply to the Bi 2:2:1:2 planes more accurately than the minimal model of Eq. (1), though less perfectly than a model parametrized for the 2:2:1:2 structure (this parametrization is not yet available). The renormalized band structure is seen to be in broad agreement with the mean-field calculations, in support of our assumption of a heavy-fermion normal state.

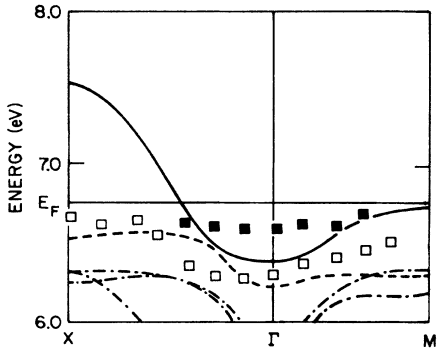

FIG. 1. Dispersion of quasiparticle bands (a) according to present calculation (solid, dotted, and dashed-dotted curves) and (b) according to the angle-resolved photoemission data of Ref. 6 (solid and open squares).

We now turn to the main task of this paper, a calculation of the inverse photoemission spectrum, working to order $1/N$ in order to describe the satellite structures which are absent in the leading order calculation. For this purpose here we use the simplified ALM[9–14] of Eqs. (1)–(5). The calculations with the full model of Ref. 5 do not differ in principle, but are exceedingly complex, and we hope eventually to report on them elsewhere. The simplified model has been optimized to be as realistic as possible, but inevitable deviations occur, most noticeably in that the mass renormalization is rather energy dependent in the simple model, while the band containing the Fermi level has a rather energy-independent mass renormalization in the full model.

The angle-integrated inverse photoemission spectrum is approximated by the spectral density of the one particle D-electron Green's function

$$\Gamma(\tau)=-\langle Tb_i^{\dagger}(0)D_i(0)b_i(\tau)D_i^{\dagger}(\tau)\rangle\,.$$

$\Gamma(iv_n)$ is calculated from the expression

$$\Gamma(iv_n)=\langle b\rangle_0^2/[G_d^{-1}(iv_n)-(iv_n-\epsilon_d)^2\langle b\rangle_0^{-2}S(iv_n)]\,. \tag{5}$$

Here $\langle b\rangle_0$ is the expectation value of b to leading order in $1/N$ (mean-field approximation), G_d is the mean-field d-propagator (defined below), and S is a self-energy given

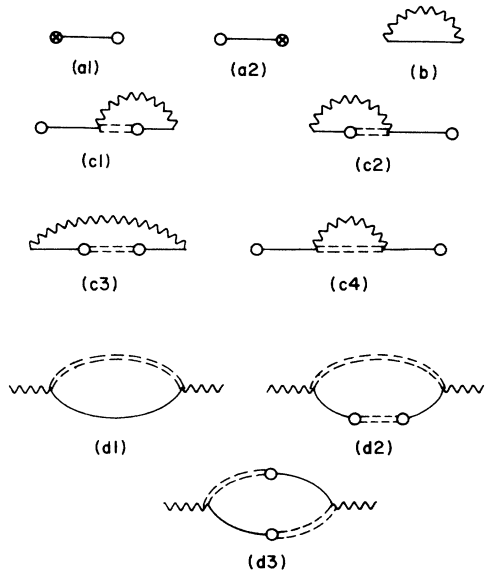

FIG. 2. (a)–(c) Diagrams for the self-energy $S(iv_n)$ in (5) to order $1/N$. Open circle, $\langle b\rangle_0$, circle with cross, order $1/N$ correction to $\langle b\rangle$. Full line, G_d^0, double-dashed line, G_k, wavy line, complete b-propagator defined in (6). (d) Self-energies of b boson to leading order in $1/N$.

by the graphs in Figs. 2(a)–2(c), which are systematic to order $1/N$. Graphs (c), taken together, are infrared regular. Graphs (a) involve the $O(1/N)$ correction to $\langle b \rangle$,[10] which is such as to cancel the infrared singularity in graph (b).[10] In a simplification appropriate in calculating angle-averaged spectra, we have defined S as the k sum of the graphs in Figs. 2(a)–2(c), and G_d also as a k sum (see below). To set this work in context, extensive calculations of photoemission and inverse photoemission spectra for single impurities exist, though mostly by other techniques;[15–17] however, for a single impurity a calculation along the present lines has been done by Coleman[13] (although in radial gauge).

The key ingredient is the b-boson propagator $D_{ij}(\tau) = -\langle T b_i(0) b_j^\dagger(\tau) \rangle$, for which extensive approximate analytic calculations are available.[9–12] A Feynman perturbation expansion in powers of V may be developed starting from Eq. (2). Summing all tadpole graphs replaces the bare fermion propagators by propagators belonging to the mean-field Hamiltonian (4),

$$G_{\mathbf{k}}(i\nu_n) = [i\nu_n - \epsilon_{\mathbf{k}} - zV_{\mathbf{k}}^2 G_d^0(i\nu_n)]^{-1},$$

$$G_{\mathbf{k}d}(i\nu_n) = bV_{\mathbf{k}} G_d^0(i\nu_n) G_{\mathbf{k}}(i\nu_n),$$

and

$$G_d(i\nu_n) = \sum_{\mathbf{k}} [G_d^0(i\nu_n) + zV_{\mathbf{k}}^2 G_{\mathbf{k}}(i\nu_n) G_d^0(i\nu_n)^2],$$

where

$$G_d^0(i\nu_n) = (i\nu_n - \epsilon_d)^{-1}.$$

Starting from Eq. (2), which generates results in the Cartesian gauge,[10,11,14] we get the bare boson propagator

$$D_{11}^0 = (i\omega_n + is - \lambda)^{-1},$$

$$D_{22}^0 = (-i\omega_n - is - \lambda)^{-1},$$

$$D_{12}^0 = D_{21}^0 = 0.$$

The expressions for the self-energies of the b boson to leading order in $1/N$, derived from the diagrams of Fig. 2(d), lead after some manipulation (and confining ourselves to the isotropic model[4] $V_{\mathbf{k}} = V$), to the formulas for the b-boson propagator[10]

$$D_{11}(q,i\omega_n) = \{-i\omega_n[1 - P_1(q,-i\omega_n)] - P_A(q,i\omega_n)\}/\Delta, \tag{6a}$$

$$D_{22}(q,i\omega_n) = \{i\omega_n[1 - P_1(q,i\omega_n)] - P_A(q,i\omega_n)\}/\Delta, \tag{6b}$$

$$D_{12}(q,i\omega_n) = D_{21}(q,i\omega_n) = P_A(q,i\omega_n)/\Delta, \tag{6c}$$

where

$$\Delta = -(i\omega_n)^2\{[1 - P_1(\omega_n)][1 - P_1(-i\omega_n)] - P_d P_A/b^2V^2\}. \tag{6d}$$

Here the polarizabilities are (notation similar to Ref. 10)

$$P_A(q,i\omega_n) = NV^2T \sum_{k,m} G_{dk}(k+q, i\omega_n + i\nu_m) \times G_{dk}(k, i\nu_m), \tag{7a}$$

$$P_1(q,i\omega_n) = (-NVT/b) \sum_{k,m} G_{dd}(k+q, i\omega_n + i\nu_m) \times G_{dk}(k, i\nu_m), \tag{7b}$$

$$P_d(q,i\omega_n) = NV^2T \sum_{k,m} G_{dd}(k+q, i\omega_n + i\nu_m) \times G_{dd}(k, i\nu_m). \tag{7c}$$

We calculated the polarizabilities in Eq. (7) by the analytical triangle method. Numerous checks have been carried out, indicating no error greater than 0.5%. An example is the dynamic charge susceptibility $\chi_{ij}^C(\tau) = -\langle T n_{di}(0) n_{di}(\tau) \rangle$, which to leading N is

$$\chi^C(q,i\omega_n) = V^{-2}\omega_n^2 P_d/\Delta.$$

In the limit $q \to 0$, $i\omega_n \to 0$, χ^C must reduce to the static charge susceptibility $\chi^C = \partial\langle n_d \rangle/\partial E_1$ at constant μ, which is 0.198 eV^{-1} with the parameters $V = 2$ eV, $D = 2.2$ eV, and $E_1 = -3.8$ eV of Fig. 5 of Ref. 4.

Using numerical calculations of (7), the spectral densi-

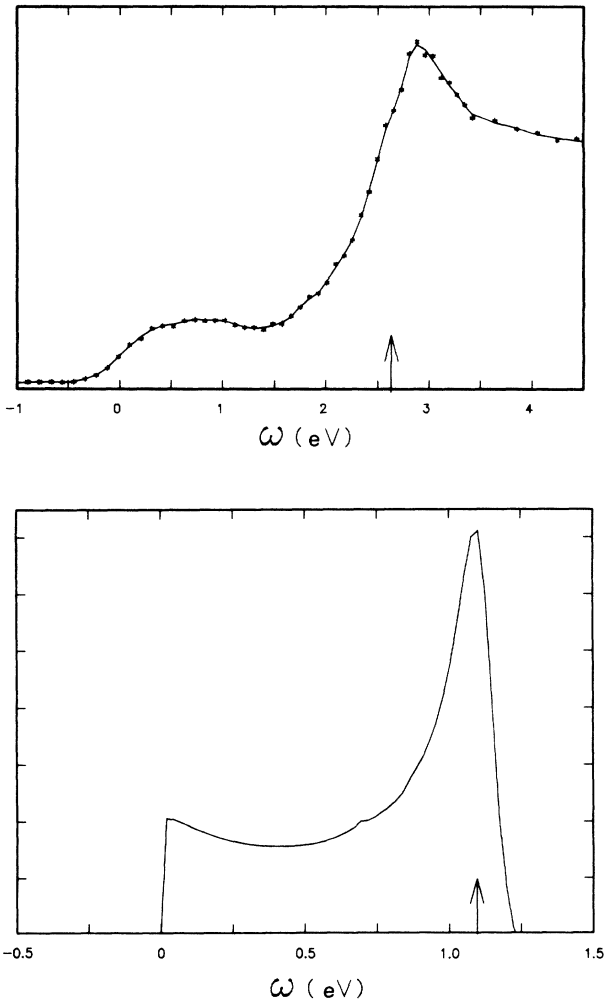

FIG. 3. Top panel, inverse photoemission spectrum of 2:2:1:2 material from Ref. 7. Bottom panel, spectral density of D Green's function to $O(1/N)$ as calculated in this paper (ordinates in arbitrary units). $x = 0.1$.

ty of the D Green's function is illustrated in Fig. 3, with recent experimental data[7] for comparison. The comparison involves no fitting parameters and is seen to be good as regards the shape of the spectrum, considering that the calculation lacks the experimental lifetime broadening, although the energy of the satellite is too low. That the discrepancy in the energy of the satellite is attributable to the difference between the oxide gap E_1 in the isotropic and the realistic models needed to get the same effective mass is seen by scaling the position of the satellite peak by a shift equal to the difference between the values of $E_1 - \epsilon_F$ in the two-band model of Ref. 4 and the 32-band model of Ref. 5. Then the peak position (vertical arrow in lower panel of Fig. 3) would appear at an energy close to the experimental peak (arrow in upper panel of Fig. 3). With this adjustment the parameter-free calculation predicts the inverse photoemission spectrum rather well.

In conclusion, we see that four features of the photoemission and inverse photoemission data on $Bi_2Sr_2CaCu_2O_8$ favor a heavy-fermion picture of the normal state: the Fermi edge, the quasiparticle band structure, the width of the empty part of the conduction band, and the inverse-photoemission satellite.

Note added in proof. Recently, we received a copy of an unpublished work by C. Melo and S. Doniach describing a somewhat similar calculation of the angle-averaged photoemission and inverse-photoemission spectra. The chief differences from the present work are (i) these authors do not employ our self-energy summation technique, (ii) their parameter choice yields a heavy quasiparticle mass, going to infinity at half filling, a choice we believe to be unphysical.

[1]P. W. Anderson, Science **235**, 1196 (1987); P. W. Anderson, G. Baskaran, Z. Zhou, and T. Hsu, Phys. Rev. Lett. **58**, 2790 (1987); G. Baskaran and P. W. Anderson, Phys. Rev. B **37**, 580 (1988).

[2]R. B. Laughlin, Phys. Rev. Lett. **60**, 2677 (1988).

[3]G. Kotliar, P. A. Lee, and N. Read, Physica C **153-155**, 538 (1988).

[4]D. M. Newns, M. Rasolt, and P. Pattnaik, Phys. Rev. B **38**, 6513 (1988).

[5]D. M. Newns, M. Rasolt, P. Pattnaik, and D. A. Papaconstantopoulos, Phys. Rev. B **38**, 7033 (1988).

[6]T. Takahashi, H. Matsuyama, H. Katayama-Yoshida, Y. Okabe, S. Hosoya, K. Seki, H. Fujimoto, M. Sato, and H. Inokuchi (unpublished).

[7]W. Drube, F. J. Himpsel, G. V. Chandrasekhar, and M. W. Shafer (unpublished); F. J. Himpsel, G. V. Chandrasekhar, A. B. McLean, and M. W. Shafer, Phys. Rev. B **38**, 11946 (1988).

[8]That this feature is intrinsic to the conduction band of the plane regions in the structure is confirmed by its duplication in the O $1s \rightarrow$ O $2p$ absorption spectrum[7] (transition probabilities confine the final states to the O $2p$, while the absence of available empty oxygens other than in the in-plane $2p$'s confines the final states to the plane).

[9]N. Read, J. Phys. C **18**, 2651 (1985).

[10]A. J. Millis and P. A. Lee, Phys. Rev. B **35**, 3394 (1987).

[11]N. Read and D. M. Newns, J. Phys. C **16**, 3273 (1983); D. M. Newns and N. Read, Adv. Phys. **36**, 799 (1987).

[12]A. Auerbach and K. Levin, Phys. Rev. Lett. **57**, 877 (1986).

[13]P. Coleman, Phys. Rev. B **28**, 5255 (1983); **29**, 3035 (1984); **35**, 5072 (1984).

[14]A. Houghton, N. Read, and H. Won, Phys. Rev. B **37**, 3782 (1988).

[15]O. Gunnarsson and K. Schonhammer, Phys. Rev. B **31**, 4815 (1985); **28**, 4315 (1983).

[16]H. Eskes and G. A. Sawatzky, Phys. Rev. Lett. **12**, 1415 (1988).

[17]J. F. Annett, R. M. Martin, A. K. Mahan, and S. Satpathy (unpublished).